Geosci. Model Dev. Discuss., 6, 5947–5980, 2013
www.geosci-model-dev-discuss.net/6/5947/2013/
doi:10.5194/gmdd-6-5947-2013

Geoscientific Model Development Discussions
Open Access

Earth Orbit v2.1: a 3-D visualization and analysis model of Earth's orbit, Milankovitch cycles and insolation

T. S. Kostadinov[1,2] **and R. Gilb**[1]

[1]Department of Geography and the Environment, 28 Westhampton Way, University of Richmond, Richmond, VA 23173, USA
[2]Formerly at Earth Research Institute, University of California Santa Barbara, Santa Barbara, CA 93106, USA

Received: 4 October 2013 – Accepted: 4 November 2013 – Published: 28 November 2013

Correspondence to: T. S. Kostadinov (tkostadi@richmond.edu)

Published by Copernicus Publications on behalf of the European Geosciences Union.

Abstract

Milankovitch theory postulates that periodic variability of Earth's orbital elements is a major climate forcing mechanism, causing, for example, the contemporary glacial-interglacial cycles. There are three Milankovitch orbital parameters: orbital eccentricity, precession and obliquity. The interaction of the amplitudes, periods and phases of these parameters controls the spatio-temporal patterns of incoming solar radiation (insolation) and the timing of the seasons with respect to perihelion. This complexity makes Earth–Sun geometry and Milankovitch theory difficult to teach effectively. Here, we present "Earth Orbit v2.1": an astronomically precise and accurate model that offers 3-D visualizations of Earth's orbital geometry, Milankovitch parameters and the ensuing insolation forcing. The model is developed in MATLAB® as a user-friendly graphical user interface. Users are presented with a choice between the Berger (1978a) and Laskar et al. (2004) astronomical solutions for eccentricity, obliquity and precession. A "demo" mode is also available, which allows the Milankovitch parameters to be varied independently of each other, so that users can isolate the effects of each parameter on orbital geometry, the seasons, and insolation. A 3-D orbital configuration plot, as well as various surface and line plots of insolation and insolation anomalies on various time and space scales are produced. Insolation computations use the model's own orbital geometry with no additional a priori input other than the Milankovitch parameter solutions. Insolation output and the underlying solar declination computation are successfully validated against the results of Laskar et al. (2004) and Meeus (1998), respectively. The model outputs some ancillary parameters as well, e.g. Earth's radius-vector length, solar declination and day length for the chosen date and latitude. Time-series plots of the Milankovitch parameters and EPICA ice core CO_2 and temperature data can be produced. Both research and pedagogical applications are envisioned for the model.

GMDD

6, 5947–5980, 2013

1 Introduction

The astrophysical characteristics of our star, the Sun, determine to first order the continuously habitable zone around it (Kasting et al., 1993; Kasting, 2010), in which rocky planets are able to maintain liquid water on their surface and sustain life. The surface temperature of a planet depends to first order upon the incoming flux of solar radiation (insolation) to its surface. Additionally, energy for our metabolism (and most of modern economy) is obtained exclusively from the Sun via the process of oxygenic photosynthesis performed by green terrestrial plants and marine phytoplankton. The high oxygen content of Earth's atmosphere, necessary for the evolution of placental mammals (Falkowski et al., 2005), is due to billions of years of photosynthesis and the geological burial of reduced carbon equivalents (Falkowski and Godfrey, 2008; Falkowski and Isozaki, 2008; Kump et al., 2010). Thus, the Sun is central to climate formation and stability and to our evolution and continued existence as a species.

The temporal and spatial patterns of insolation and their variability on various scales determine climatic stability over geologic time, as well as climate characteristics such as diurnal, seasonal and pole to Equator temperature contrasts, all of which influence planetary habitability. Insolation can change due to changes in the luminosity of the Sun itself. This can happen due to the slow increase of solar luminosity that gives rise to the Faint Young Sun Paradox (Kasting, 2010; Kump et al., 2010), or it can happen on much shorter time scales such as the 11 yr sunspot cycle (Fröhlich, 2013; Hansen et al., 2013). Importantly, insolation is also affected by the orbital elements of the planet. According to the astronomical theory of climate, periodical variations in Earth's orbital elements cause multi-millennial variability in the spatio-temporal distributions of insolation, and thus provide an external forcing and pacing to Earth's climate, for example causing the glacial-interglacial cycles of the Quaternary (Milankovitch, 1941; Berger, 1988; Berger and Loutre, 1994). These periodic orbital fluctuations are called Milankovitch cycles, after the Serbian mathematician Milutin Milankovitch who was instrumental in developing the theory (Milankovitch, 1941). There are three

GMDD
6, 5947–5980, 2013

Milankovitch orbital parameters: orbital eccentricity (main periodicities of ~ 100 000 and ~ 400 000 yr), precession (quantified as the longitude of perihelion, main periodicities ~ 19 000–23 000 yr) and obliquity of the ecliptic (main periodicity 41 000 yr) (Berger, 1978a). The pioneering work by Hays et al. (1976) demonstrated a strong correlation between these cycles and paleoclimatological records. Since then, multiple analyses of paleoclimate records have been found to be consistent with Milankovitch forcing (e.g. Imbrie et al., 1992; Rial, 1999; Lisiecki and Raymo, 2005). However, some controversies remain, notably the 100 Ky problem (e.g. Imbrie et al., 1993; Loutre et al., 2004; Berger et al., 2005). Predicting the Earth system response to orbital forcing is not trivial, and there are challenges in determining which insolation quantity (i.e. integrated over what time and space scales) is responsible for paleoclimate change (Imbrie et al., 1993; Lisiecki et al., 2008; Huybers, 2006). Alternative theories have also been proposed, such as the influence of the orbital inclination cycle (Muller and McDonald, 1997).

The Milankovitch cycles are due to complex gravitational interactions between the bodies of the solar system. Astronomical solutions for the values of the Milankovitch orbital parameters have been derived for several tens of million years into the past and future, notably by Berger (1978a, b), referred to henceforth as Be78, and Laskar et al. (2004), referred to henceforth as La2004. Solutions are also provided by Berger and Loutre (1992) and Laskar et al. (2011). These astronomical solutions are crucial for paleoclimate and climate science, as they enable the computation of insolation at any latitude and time period in the past or future within the years spanned by the solutions (Berger and Loutre, 1994; Berger et al., 2010; Laskar et al., 2004), and subsequently the use of this insolation in climate models as forcing (e.g. Berger et al., 1998). Climate models are an important method for testing the response of the Earth system to Milankovitch forcing.

While most Earth science students and professionals are well aware of Earth's orbital configuration and the basics of the Milankovitch cycles, the details of both and the way the Milankovitch orbital elements influence spatio-temporal patterns of insolation on

GMDD
6, 5947–5980, 2013

various time and space scales remain elusive. It is difficult to appreciate the pivotal importance of Kepler's laws of planetary motion in controlling the effects of Milankovitch cycles on insolation patterns. The three-dimensional nature of Earth's orbit, the vast range of space and time scales involved, and the geometric details are complex, and yet those same factors present themselves to computer modeling and 3-D visualization. Here, we present "Earth Orbit v2.1": an astronomically precise and accurate 3-D visualization and analysis model of Earth's orbit, Milankovitch cycles, and insolation. The model is envisioned for both research and pedagogical applications and offers 3-D visualizations of Earth's orbital geometry, Milankovitch parameters and the ensuing insolation forcing. It is developed in MATLAB® and has an intuitive, user-friendly graphical user interface (GUI) (Fig. 1). Users are presented with a choice between the Be78 and La2004 astronomical solutions for eccentricity, obliquity and precession. A "demo" mode is also available, which allows the three Milankovitch parameters to be varied independently of each other (and exaggerated over much larger ranges than the naturally occurring ones), so users can isolate the effects of each parameter on orbital geometry, the seasons, and insolation. Users select a calendar date and the Earth is placed in its orbit using Kepler's laws; the calendar can be started on either vernal equinox (20 March) or perihelion (3 January). A 3-D orbital configuration visualization, as well as spatio-temporal surface and line plots of insolation and insolation anomalies (with respect to J2000) on various scales are then produced. Below, we first describe the model parameters and implementation. We then detail the model user interface, provide instructions on its capabilities and use, and describe the output. We then present successful model validation results, which are comparisons to existing independently derived insolation, solar declination and season length values. Finally, we conclude with brief analysis of sources of uncertainty. Throughout, we provide examples of the pedagogical value of the model.

Various insolation solutions and visualizations exist (Berger, 1978a; Rubincam, 1994 however, see response of Berger, 1996; Laskar et al., 2004; Archer, 2013; Huybers, 2006). The model presented here computes insolation from first principles of orbital

GMDD
6, 5947–5980, 2013

mechanics (Kepler's laws) and irradiance propagation and using exclusively its own internal geometry. The only model inputs are the three Milankovitch orbital parameters, either real astronomical solutions (Be78 or La2004) or user-entered demo values. No insolation computation logic from the above-cited existing solutions has been used, so comparison with these solutions constitutes independent model verification, referred to here as validation, because we consider the La2004 and Meeus (1998) solutions the geophysical truth (Sect. 5).

The unique contribution of our model consists of the combination of the following features: (a) central to the whole model is a user-controllable, 3-D pan-tilt-zoom plot of the actual Earth orbit, (b) an interactive user-friendly GUI that serves as a single-entry control panel for the entire model and makes it suitable for use by non-programmers and friendly to didactic applications, (c) the Milankovitch cycles are incorporated explicitly and insolation is output according to real or user-selected demo orbital elements, which (d) allows users to enter exaggerated orbital parameters independently of each other and isolate their effects on insolation, as well as view the orbit with exaggerated eccentricity and (e) the source code is published and advanced users can check its logic, as well as modify it and adapt it.

The issue of climate change has come to the forefront of Earth science and policy and it is arguably the most important global issue of immediate and long-term consequences. Earth's climate varies naturally over multiple time scales, from decadal to hundreds of millions of years (e.g. Kump et al., 2010). It is thus crucial to understand natural climate forcings, their time scales, and the ensuing response of the Earth system. In addition, detailed understanding of the Sun's daily path in the sky and the patterns of insolation have become important to increasing numbers of students and professionals because of the rise in usage of solar power (thermal and photovoltaic). We submit that the model presented here can enhance understanding of all of these important subject areas.

GMDD
6, 5947–5980, 2013

2 Key definitions, model parameters and implementation

The model input parameters, and their values and units, are summarized in Table 1. The following definitions, discussion and symbols are consistent with those of Berger et al. (2010). The reader is referred to their Fig. 1. According to Kepler's First Law of Planetary Motion, Earth's orbit is an ellipse, and the Sun is in one of its foci (e.g. Meeus, 1998). Orbital eccentricity, e (Table 1), is a measure of the deviation of Earth's orbital ellipse from a circle and is defined as $e = \sqrt{1 - b^2/a^2}$, where a is the semi-major axis (Table 1) and b is the semi-minor axis of the orbital ellipse (e.g. Berger and Loutre, 1994). The semi-major axis is about equal to 1 AU (Meeus, 1998; Standish et al., 1992) and determines the size of the orbital ellipse and thus the orbital period of Earth; it is considered a fixed constant in the model, as its variations are extremely small (Berger et al., 2010; Laskar et al., 2004, their Fig. 11). Various orbital period definitions are possible; here, the sidereal period is used as a model constant (Meeus, 1998). Thus, Kepler's Third Law of Planetary Motion is implicit in these two constant definitions and is not included explicitly elsewhere in model logic. The obliquity of Earth, ε, is the angle between the direction of its axis of rotation and the normal to the orbital plane, or the ecliptic (Table 1). Eccentricity and obliquity are two of the three Milankovitch orbital parameters.

The third Milankovitch orbital parameter, precession, is the most challenging for instruction and visualization. There are two separate kinds of precession that combine to create a climatic effect – precession of the equinoxes (also termed axial precession), and apsidal precession, i.e. precession of the perihelion in the case of Earth's orbit. Axial precession refers to the wobbling of Earth's axis of rotation that slowly changes its absolute orientation in space with respect to the distant stars. The axis or rotation describes a cone (one in each hemisphere) in space with a periodicity of about 26 000 yr (Berger and Loutre, 1994). This is the reason why the star α UMi (present-day Polaris, or the North Star), has not and will not always be aligned with the direction of the North Pole. Also, due to axial precession, the point of vernal equinox in the sky moves with

GMDD
6, 5947–5980, 2013

respect to the distant stars and occurs in successively earlier zodiacal constellations. Axial precession is clockwise as viewed from above the North Pole, hence the North Celestial Pole describes a counter-clockwise motion as viewed by an observer looking in the direction of the North Ecliptic Pole. Precession of the perihelion refers to the gradual rotation of the line joining aphelion and perihelion, with respect to the distant stars (or the reference equinox of a given epoch) (Berger, 1978a; Berger and Loutre, 1994).

Axial precession and precession of the perihelion combine to modulate the *relative* position of the equinoxes and solstices (i.e. the seasons) with respect to perihelion, which is what is relevant for insolation and climate. This climatically-relevant precession is implemented in the model and is quantified via the longitude of perihelion, $\tilde{\omega}$, which is the angle between the directions of the moving fall equinox and perihelion at a given time, measured counterclockwise in the plane of the ecliptic (Berger et al., 2010). Because both perihelion and equinox move, the longitude of perihelion will have a different (shorter) periodicity than one full cycle of axial wobbling alone (Berger and Loutre, 1994). The direction of Earth's radius-vector when Earth is at fall equinox ($\sim$ 22 September) is referred to as the direction of fall equinox above. This is the direction with respect to the distant stars where the Sun would be found on its annual motion on the ecliptic on 20 March – i.e. at vernal equinox. In other words, that is the direction of the vernal point in the sky (Berger et al., 2010, their Fig. 1 and Appendix B), the origin of the right ascension coordinate. This distinction between vernal equinox and the direction of the vernal point can cause confusion, especially since the exact definition of longitude of perihelion can vary (e.g. c.f. Berger et al., 1978a, 1993, 2010; Berger and Loutre, 1994; Joussaume and Braconnot, 2007) and the longitude of perihelion can also be confused with the longitude of perigee, $\varpi = \tilde{\omega} + 180^{\circ}$ (Berger et al., 2010). Here, we use the terminology and definitions of Berger et al. (2010).

The magnitude of the climatic effect of precession is modulated by eccentricity. In the extreme example, if eccentricity were exactly zero, the effects of precession would be null. Climatic precession, $e \sin \varpi$, is the parameter that quantifies precession and

GMDD
6, 5947–5980, 2013

determines season lengths, the Earth–Sun distance at summer solstice (Berger and Loutre, 1994) and various important insolation quantities (Berger et al., 1993, their Table 1). This interplay between eccentricity and precession presents an important way to introduce both concepts pedagogically and to test student comprehension.

The solar "constant", S_0, is defined here as the total solar irradiance (TSI) on a flat surface perpendicular to the solar rays at a reference distance of exactly 1 AU (Table 1). As Berger et al. (2010) note, due to eccentricity changes, the mean distance from the Earth to the Sun over a year is not constant on geologic time scales (it also matters how the mean is defined – e.g. over time (mean anomaly) vs. over true anomaly). If S_0 is defined to be the irradiance from the Sun at the mean Earth–Sun distance, then it is indeed not a true constant. As used here, S_0 is a true model constant as long as the luminosity of the Sun itself is assumed constant. The default value is chosen to be $1366\,\mathrm{W\,m^{-2}}$ (Fröhlich, 2013). Recent evidence suggests that the appropriate value may actually be about $1361\,\mathrm{W\,m^{-2}}$ (Kopp and Lean, 2011). Users can change the value of S_0 independently of other model inputs in order to study the effects of changes in absolute solar luminosity – e.g. in order to simulate the Faint Young Sun (e.g. Kasting, 2010) or the sunspot cycle (e.g. Hansen, 2013).

2.1 Model coordinate system; Sun–Earth geometry parameterization; solar declination

The model uses a heliocentric Cartesian coordinate system and parameterizes the orbital ellipse with one of its foci (where the Sun is) at the origin of the coordinate system. Given a date, true anomaly, ν, is determined by solving the inverse Kepler equation (see Sect. 2.2 below). The planet's radius vector can then be solved for, as true anomaly determines its direction and its magnitude is given by (Meeus, 1998):

$$|\boldsymbol{r}| = \frac{a(1-e^2)}{1+e\cos\nu} \tag{1}$$

GMDD
6, 5947–5980, 2013

The Earth is plotted in a Cartesian coordinate system (origin at Earth's center) as a sphere parameterized in terms of its radius and geographic latitude and longitude (corresponding to the two angles of a spherical coordinate system). The Earth's coordinate system's x and y axes are in the plane of the Equator (shown as a black dotted line, Fig. 2), and its z axis is pointing towards the true North Pole and is coinciding with Earth's axis of rotation; these axes are also plotted in black dotted lines, the z axis is lengthened toward North so that it pierces Earth's surface and is labeled, since this is critical in the definition and understanding of the seasons. Earth is plotted as a transparent mesh so that important orbital elements can be seen through it at various zoom levels (Fig. 2). The color scale of Earth's mesh is just a function of latitude and no day and night sides are explicitly shown. Earth's radius is not to scale with the orbit itself or with the Sun's radius. Thus, the center of Earth has its true geometric orbital position (and is the tip of its instantaneous radius-vector); however the surface of the sphere in the model is arbitrary and must not be interpreted as the true surface onto which insolation is computed, for example. The insolation computations (Sect. 2.3) are geocentric. The Sun is also plotted (not to scale) as a sphere centered at the origin of the model coordinate system.

The Earth is oriented properly in 3-D with respect to the orbital ellipse by using a rotation matrix to rotate its coordinate system. The 3-D rotation matrix is computed using Rodrigues' formula (Belongie, 2013) for 3-D rotation about a given direction by a given angle. The direction about which Earth is rotated is determined by a vector which is always in the orbital plane ($\boldsymbol{k}$-component is zero), and the $\boldsymbol{i}$ and $\boldsymbol{j}$ components are determined by the longitude of perihelion. The angle by which Earth is rotated is determined by obliquity. Thus, the rotation matrix is a function of two of the three Milankovitch parameters and is a valuable and useful instructional tool/concept for lessons in geometry, mathematics, astronomy, physical geography, and climatology. At this point the Earth is correctly oriented in 3-D space with respect to its orbit and the distant stars. Earth is then translated to its proper instantaneous position on its orbit by addition of its radius-vector to all relevant Earth-bound model elements.

GMDD
6, 5947–5980, 2013

Declination is one of the two spherical coordinates of the equatorial astronomical coordinate system. It is measured along a celestial meridian (hour circle) and is defined as the angle between the celestial Equator and the direction toward the celestial object (Meeus, 1998). Solar declination varies with the seasons, due to obliquity. It is zero at the equinoxes, reaches a maximum of $+\varepsilon$ at summer solstice and a minimum of $-\varepsilon$ at winter solstice. Solar declination determines the length of day and the daily path of the Sun in the sky at a given latitude, i.e. its altitude and azimuth above the horizon as a function of time. Thus, solar declination determines instantaneous and time-integrated insolation. In turn, solar declination and its evolution over the course of a year are a function of the orbital elements; thus it provides the mathematical and conceptual link between the Milankovitch orbital elements and insolation and climate. Here, we compute instantaneous solar declination using the angle between the direction of the North Pole and Earth's radius-vector, calculated using their dot product. Thus, we explicitly compute solar declination from the geometry of the model and it is a model *emergent property* rather than prescribed a priori; therefore, this also applies to insolation computations (Sects. 2.3 and 5).

2.2 Implementation of Kepler's Second Law of planetary motion

The heliocentric position of a planet in an elliptical orbit at a given instant of time is given in terms of its true anomaly, ν – the angle between the directions of perihelion and the radius-vector of the planet, subtended at the Sun and measured counter-clockwise in the plane of the orbit. In other words, true anomaly is the angle which the planet has "swept" from its orbit since last perihelion passage. Kepler's Second Law of planetary motion states that the planet will "sweep" equal areas of its orbit in equal intervals of time and governs the value of true anomaly as a function of time (e.g. Meeus, 1998; Joussaume and Braconnot, 1997). At non-zero eccentricity, ν is not simply proportional to time since last perihelion passage (time of flight) expressed as a fraction of the orbital period in angular units. The latter quantity is called mean anomaly, M. Kepler's Second Law is used to relate M and ν, using an auxiliary quantity called eccentric anomaly, E.

GMDD
6, 5947–5980, 2013

E and M are related by Kepler's Equation (Meeus, 1998):

$$E = M + e \sin E, \tag{2}$$

where e is orbital eccentricity. When E is known, v can be solved for using (Meeus, 1998):

$$\tan \frac{v}{2} = \sqrt{\frac{1+e}{1-e}} \tan \frac{E}{2} \tag{3}$$

The forward Kepler problem consists of solving for time of flight, M, given the planetary position, v. This is straightforward by first solving for E in Eq. (3) and using it to solve for M in Eq. (2).

However, in the most intuitive case, which is implemented here, the user enters a desired date, and the position of the planet has to be determined from the date, i.e. time of flight/mean anomaly M is given, and true anomaly has to be determined. This is referred to as the inverse Kepler problem and amounts to solving for E in Eq. (2) and then for v in Eq. (3). Solving for E is not straightforward, as no analytical solution exists. Numerous numerical methods exist for the solution of the inverse Kepler problem. Here, the binary search algorithm of Sinnott et al. (1985) is used, as given in Meeus (1998). It has the advantage of being computationally efficient, which becomes important when time series of insolation is the desired model output. It also has the distinct advantages of being valid for any value of eccentricity and converging to the exact solution to within the user machine's precision.

2.3 Implementation of insolation computation

Instantaneous insolation at the top of the atmosphere (TOA) can be computed as:

$$S(h, \boldsymbol{r}) = S_o \left(\frac{|\boldsymbol{r}_o|}{|\boldsymbol{r}|} \right)^2 \sin h, \tag{4}$$

GMDD
6, 5947–5980, 2013

where $|\boldsymbol{r}|$ is the length of the radius-vector of Earth expressed in AU, and h is the altitude of the Sun above the horizon (e.g. Berger et al., 2010). Equation (4) is an expression of the inverse square law and Lambert cosine law of irradiance. The radius-vector length is computed in the model for the chosen date (and not for every instant) using Eq. (1). S_o is the TSI at $|\boldsymbol{r}_o| = 1$ AU by definition (Sect. 2). In this equation insolation, S, is defined as the total (spectrally integrated) solar radiant energy impinging at the TOA on a unit surface area parallel to the mathematical horizon at a given latitude at a given instant. S carries the units of S_o, here $\mathrm{W\,m^{-2}}$. S needs to be integrated over time and/or space in order to compute insolation quantities of interest. Here, the main discrete time step over which S is computed and output is one 24 h period, i.e. daily insolation.

Daily insolation is a function of latitude, date, and S_o. The date is associated with a given true anomaly for a given calendar start date and orbital configuration (Joussaume and Braconnot, 1997; Sect. 2.3.1). This determines the current solar declination and the length of the radius-vector of Earth, i.e. the Sun–Earth distance. The user inputs the desired latitude, date and TSI, and the rest of the quantities are computed from the model geometry. Solar declination and the latitude determine the daily evolution of solar altitude, h, as a function of time, as follows (e.g. Meeus, 1998):

$$\sin h = \sin\delta \sin\phi + \cos\delta \cos\phi \cos t \tag{5}$$

In the above equation δ is solar declination, ϕ is geographic latitude on Earth, and t is the hour angle of the Sun. δ is assumed constant for the day of interest, and t is a measure of the progress of time. Half the day length, t_s, (i.e. the time between local solar noon and sunset), is determined by setting $h = 0^\circ$ in Eq. (5):

$$t_s = \mathrm{acos}(-\tan\phi \tan\delta) \tag{6}$$

GMDD
6, 5947–5980, 2013

Equation (5) is integrated over time from solar noon to sunset in order to compute the time-average of the sine of the solar altitude for the given date and latitude:

$$\sin h\_ave = \frac{1}{t_s}\int_0^{t_s}(\sin\delta\sin\phi + \cos\delta\cos\phi\cos t)dt \quad (7)$$

Equation (7) is integrated numerically with a very small time step of about 10 s. Because the altitude of the Sun is symmetric about solar noon, it is sufficient to integrate only from solar noon to sunset time. Daily insolation is then computed by using the time-averaged sinh_ave quantity in Eq. (4). The results are scaled by multiplying by the actual day length and dividing by 24 h. The resulting quantity represents the mean daily insolation over a full day, which is the standard value used in astronomical, climate and paleoclimate science (e.g. Laskar, 2013). If this daily insolation is multiplied by 24 h (in seconds), total energy receipt for that day (in $J\,m^{-2}$) can be calculated.

At high latitudes, there are periods of the year with no sunset or no sunrise. These cases depend on the relationship of latitude and solar declination (e.g. Berger et al., 2010). They are handled separately by either integrating Eq. (7) over 24 h, or, in the case of no sunrise (polar night), assigning a value of exactly $0\,W\,m^{-2}$ to daily insolation.

2.3.1 Integrating insolation over longer time periods – caveats

Because of the varying eccentricity and longitude of perihelion, there is no fixed correspondence between true anomaly and any one single calendar date, even if one were to define a fixed calendar start date. True anomaly and longitude are the astronomically rigorous ways to define a certain moment in Earth's year and seasons (e.g. Berger et al., 2010). If one wishes to make insolation comparisons between different orbital configurations, one must define strictly a calendar start date, and even then insolation will be in phase for different geological periods only for that date (Joussaume and Braconnot, 1997). Thus, the question "What is insolation on 20 June?" is ill posed,

GMDD
6, 5947–5980, 2013

unless one defines strictly what is meant by the date of 20 June. The Earth orbit model presented here uses the common sense calendar dates (24 h periods) as the time input because this is much more intuitive to non-experts, and because it serves the educational purposes of the model best. The user has as a choice of calendar start date (Sect. 3) and true solar longitude is output (Sect. 4.2) to remind users of the above considerations.

The problem is exacerbated if one wishes to compare insolation integrated over periods of time longer than a day. Over geologic time scales, the interval of true anomaly "swept" between two dates is not constant, and thus the length of the seasons varies. In addition, the time step of integration can also influence the results, e.g. if annual insolation is averaged with a 5 day step, results are substantially different from the case when a 1 day step is used (not shown). For this reason, the model computes annually averaged insolation at a given latitude by using 1 day steps of integration. Finally, we note that the daily insolation computations of the model are robust and validated (Sect. 5.1); however, the model has limited functionality for making comparisons of insolation integrated over longer time periods over different geologic scales. In order to make such comparisons, the use of the elliptical integrals method of Berger et al. (2010) is recommended, as well as the Laskar (2013) methods.

3 Model user interface

The Earth orbit model is provided as Supplement (Appendix A). The model is developed and runs in MATLAB®. All model control is realized via a single, user-friendly GUI panel (Fig. 1). Users are presented with a choice between the Be78 and the La2004 astronomical solutions for eccentricity, obliquity and precession. A "demo" mode is also available. If a real astronomical solution is chosen, users are asked to input a year before or after present (defined as J2000) for which they wish to run the model. The Be78 solution is available for ±1 Myr before present, whereas the La2004 solution is available for 100 Myr in the past and 20 Myr in the future. The model then looks up the values

GMDD
6, 5947–5980, 2013

of eccentricity, obliquity and precession for the chosen year and solution, and these values are used in subsequent visualizations and analyses. If the user chooses the "demo" mode, they select, independently of each other, the values of the Milankovitch parameters, which can be greatly exaggerated. In this way users can isolate the effects of each parameter on orbital geometry, the seasons, and insolation. The "demo" mode is central to the pedagogical value and applications of the model because it allows users to build and visualize an imaginary orbit of, for example, very high eccentricity while keeping obliquity fixed. Moreover, it will output all subsequent parameters, such as solar declination, day length, radius-vector length, based on this exaggerated imaginary orbit.

Users input the desired calendar date, geographic latitude on Earth, and desired value of TSI. The calendar date defaults to the current date, latitude defaults to 43° N, and TSI defaults to 1366 $W m^{-2}$ (Sect. 2). Two choices of calendar start date are available: either fix vernal equinox to be at the beginning of 20 March (default), or fix perihelion to be at the beginning of 3 January. The availability of this choice complicates interpretation of model output; however it has high instructional value. It illustrates that the choice of calendar start date and a calendar system is a human construct, accepted by convention; it is based on the actual year and day length but is relative. This can also help test knowledge of the concepts explained in Sect. 2.3.1. The effect of the different choice of calendar start date is most apparent at exaggerated eccentricities and/or at longitudes of perihelion that are very different from the contemporary value. Insolation time series output (Sect. 4) is only computed for the calendar being fixed to vernal equinox on 20 March.

GMDD
6, 5947–5980, 2013

4 Model output

4.1 Graphical output

The main output of the model is a 3-D plot of Earth's orbital configuration. Figure 2a illustrates an example with the J2000 values of the Milankovitch parameters, according to the La2004 solution, for 16 September. Figure 2b illustrates an imaginary orbit with exaggerated eccentricity and obliquity and longitude of perihelion very different from the J2000 one. These plots have pan-tilt-zoom capability, so users can view the orbital configuration from many perspectives; this is at the core of the pedagogical value of the model. The plot is updated with the current parameter selections by pressing the "Plot/Update Orbit" button.

Users are presented with several options of plotting insolation as function of time and latitude. First, insolation can be plotted for a single year (using the currently selected Milankovitch parameters) as a function of day of year and latitude (Fig. 3a). Insolation anomalies with respect to the J2000 La2004 orbital configuration are also plotted, using $S_o = 1366\,\mathrm{W\,m^{-2}}$ (Fig. 3b). Anomalies are especially useful when analyzing the effect of changes in insolation on the glacial-interglacial cycles. For example, the anomalies at 65° N during summer months 115 000 yr BP (Fig. 3b) suggest the inception of glaciation (e.g. Joussaume and Braconnot, 1997), as these areas were receiving about 35–40 $\mathrm{W\,m^{-2}}$ less insolation than they are receiving now. The data in these plots is computed with a step of 5 days and 5° of latitude. Multi-millennial insolation time series can also be plotted in a 3-D surface plot as a function of year since J2000 and day of year, at the selected latitude. Users select the start and end years for the time series. The data for these plots are computed for steps of 1000 yr and one day (for day of year). An example of the output is provided in Fig. 3c.

Several time series line plots are also produced. Insolation time series are plotted for the currently selected latitude; both the current date and the annual average are shown (Fig. 4a). A multi-panel plot (Fig. 4b) allows the comparison of the three Milankovitch parameters. Precession is visualized as the longitude of perihelion, as well

GMDD
6, 5947–5980, 2013

as the climatic precession parameter, $e \sin \varpi$ (Berger and Loutre, 1994). The last panel of Fig. 4b shows the EPICA CO_2 (Lüthi et al., 2008a, b) and deuterium temperature (Jouzel et al., 2007a, b) time series for the last ~ 800 kyr. These paleoclimatic data illustrate clearly the last few glacial-interglacial cycles with main periodicity of ~ 100 kyr (e.g. Lisiecki and Raymo, 2005). This allows users to correlate visually these paleoclimatic time series with the corresponding Milankovitch parameter and insolation curves.

4.2 Numerical/ancillary output

Ancillary data (and their units) are output in the main GUI window (Fig. 1) and are updated every time the Earth orbit plot (Fig. 2) is re-drawn, i.e. every time the "Plot/Update Orbit" button is pressed (Sect. 4.1). Variables that are output in the main GUI are as follows: solar declination, insolation at the TOA for the chosen date and latitude, day length, Sun–Earth distance, length of the seasons (as defined in the Northern Hemisphere (NH)), the longitude of perigee, and true and mean longitude of the Sun. The longitude of perigee is the angle between the directions of vernal equinox and perihelion, measured counterclockwise as viewed from the North Pole direction, in the plane of the orbit (Berger et al., 2010; Sect. 2). The true longitude of the Sun is equal to Earth's true anomaly plus the longitude of perigee (Berger et al., 2010, their Eq. 6). True longitude is the angle Earth has swept from its orbit, subtended at the Sun, since it was last at vernal equinox. Mean longitude is the longitude of the mean Sun, in an imaginary perfectly circular orbit of the same period, i.e. mean longitude is proportional to the passage of time, much like mean anomaly. Users also are given the option of saving the data used to make the insolation plots in Fig. 3 in ASCII format. The first row and column of these files list the abscissa and ordinate values of the data, respectively.

GMDD
6, 5947–5980, 2013

5 Model validation

5.1 Insolation validation

Daily insolation is the most important model output from climate science perspective and is the fundamental discrete time unit at which the model calculates energy receipt at the TOA. Daily insolation was validated against the results of Laskar et al. (2004), as provided in Laskar (2013). Three dates were tested – 22 March, 20 June, 22 December, for the present (J2000) and for +10 000 yr since present. Validation is excellent; all test cases result in differences less than 1 $W m^{-2}$ (Fig. 5). We used the same value for TSI as Laskar (2013) – the default model value. The model uses its own internally constructed orbital geometry and first principles equations to compute insolation. There is no additional a priori prescribed constraint to the model other than the orbital elements solution and the orbital period (Sects. 2 and 2.3). Therefore the validation presented here is an independent verification of the model's geometry and computations, taking the Laskar (2013) values as truth. Section 6 discusses sources of model uncertainty which can explain some of the small differences observed. We also note that Laskar (2013) defines 21 March as spring equinox, whereas we use 20 March, so his calendar dates are offset by one with respect to the dates used here. This has been taken into account in the validation.

5.2 Solar declination validation and season length validation

Solar declination was validated against the algorithms of Meeus (1998). The model year is neither leap, nor common (Table 1) and is thus not equivalent to any single Gregorian calendar year. In order to validate declination at all dates, the Meeus (1998) algorithm was used to compute solar declinations for 12:00 UT on each date of four years (2009–2012, 2012 being leap) and average the declinations for each date (not day of year, Fig. 6). These averages were then compared to the solar declination output by the model for that date. Results indicate differences are always less than ~ 0.2°

GMDD
6, 5947–5980, 2013

(Fig. 6, black line). By construction, model solar declination on 20 March will always be exactly zero degrees. In reality, the exact instance of vernal equinox varies year to year, so these validation differences are expected. Importantly, the differences between the model and the 4 yr averaged Meeus (1998) declinations are consistently smaller than the daily rate of change of declination (Fig. 6, green curve), as computed from the Meeus (1998) data. Additionally, these differences are of a similar magnitude to the standard deviation of declination between these four years for each date (Fig. 6, red curve). Thus the solar declination validation is excellent and model configuration for each date is representative of a typical generic Gregorian calendar date. Finally, season lengths are an excellent method to validate the geometry of the model, because they test that the model is correctly computing a given time of flight on the orbit for a section of the orbit that corresponds to a given season, and generally not coinciding with special points such as perihelion. Season lengths agree to within 0.01 days with the tabulated values of Meeus (1998) (his Table 27F).

6 Sources of uncertainties

Assumptions and approximations in the model propagate to uncertainties in the model outputs, such as declination and insolation. Some of these assumptions were already discussed (e.g. Sect. 2.3.1). Here, we draw the users' attention to a few additional sources of uncertainty. Determination of some of these uncertainties is outside the scope of this work; however, users can run sensitivity analyses using the model in order to quantify them. Importantly, uncertainties in the astronomical solutions that are used as input to the model will propagate to insolation computations. Accuracy is highest near the present time and degrades further into the past or future (Laskar, 1999). The model is prescribed the sidereal year as the orbital period (Table 1), which is slightly longer than the tropical year (Meeus, 1998). The difference is of the order of 0.01 days. The use of these two different period definitions leads to negligible differences in solar declination on a given date (not shown), much smaller than the validation differences

GMDD
6, 5947–5980, 2013

of Fig. 6. We conclude that the choice of orbital period does not influence the insolation computations significantly.

A single value for solar declination and the radius-vector length is used in the computation of daily insolation (Sect. 2.3). In reality, these quantities change continuously, instead of having discrete values. This is likely to introduce small errors in insolation that will be smaller in magnitude than the difference in daily insolation between successive days. Sunrise and sunset times used in the insolation computation are referred to the center of the disk of the Sun and the mathematical horizon at the given latitude at the surface of Earth. Note also that irradiance is given at the top of the atmosphere (TOA), but all computations are geocentric, rather than topocentric, which should lead to negligible insolation differences.

Since the model year is not an integral number of days, if total annual insolation is computed by summing daily insolation values, the 19 March insolation needs to be scaled by 1.256363 to reflect the fact that this day is 24×1.256363 h long in the model (Berger et al., 2010). Here, we average daily insolation to output average annual insolation, so this correction is not applied.

7 Concluding Remarks

We presented Earth Orbit v2.1, an interactive 3-D analysis and visualization model of the Earth orbit, Milankovitch cycles, and insolation. The model is written and runs in MATLAB® and is controlled from a single integrated user-friendly GUI. Users choose a real astronomical solution for the Milankovitch parameters or user-selected demo values. The model outputs a 3-D plot of Earth's orbital configuration (with pan-tilt-zoom capability), selected insolation time series, and numerical ancillary data. The model is intended for both research and educational use. We emphasize the pedagogical value of the model and envision some of its primary uses will be in the classroom. The user-friendly GUI makes the model very accessible to non-programmers. It is also accessible to non-experts and the K-12 classroom, as minimal scientific background is

GMDD
6, 5947–5980, 2013

required to use the model in an instructional setting. Disciplines for which the model can be used span mathematics (e.g. spherical geometry, linear algebra, curve and surface parameterizations), astronomy, computer science, Earth system science, climatology and paleoclimatology, physical geography and related fields.

The authors encourage feedback and request that comments, suggestions, and reports of errors/omissions be directed to tkostadi@richmond.edu.

Appendix A

Code availability and license

The files necessary to run the model "Earth Orbit v2.1" in MATLAB® are provided here as Supplement. In addition, model files are expected to be available on the website of the University of Richmond Department of Geography and the Environment (http://geography.richmond.edu), under the *Resources* category; documented updates may be posted there. The GUI is raised by typing the name of the associated script ("Earth_orbit_v2_1.m") on the MATLAB® command line. The model has been tested in MATLAB® release R2013b on 64-bit Windows 7 Enterprise SP1 and Linux Ubuntu 12.04 LTS, but should run correctly in earlier versions of MATLAB® and on different platforms. The model is distributed under the Creative Commons BY-NC-SA 3.0 license. It is free for use, distribution and modification for non-commercial purposes. Details are provided in the ReadMe.txt file.

Supplementary material related to this article is available online at http://www.geosci-model-dev-discuss.net/6/5947/2013/gmdd-6-5947-2013-supplement.zip.

GMDD
6, 5947–5980, 2013

Acknowledgements. Funding for this work was provided to T. S. Kostadinov by the Andrew W. Mellon Foundation/Associated Colleges of the South Environmental Postdoctoral Fellowship and the University of Richmond School of Arts and Sciences. The University of Richmond School of Arts and Sciences also provided funding for R. Gilb. We would especially like to acknowledge Martin Medina for his help and the incredibly inspirational discussions. This project would not have been conceived without him. We also thank André Berger and Jacques Laskar for their Milankovitch and insolation solutions, Jacques Laskar for providing input data files for his solutions, and Gary L. Russell/NASA GISS for the Berger Milankovitch solutions code. We thank David Kitchen for the useful discussions. EPICA data set contributors are also hereby acknowledged. T. S. Kostadinov expresses his gratitude to Van Nall and Della Dumbaugh for their multivariate calculus and linear algebra classes at University of Richmond, as well as to other mathematics and computer science faculty at the University of Richmond. We thank Jean Meeus for his excellent *Astronomical Algorithms*. We also thank the Wikipedia® Project and its contributors for providing multiple articles on mathematics, astronomy, orbital mechanics, and Earth Science that are a great first step in conducting research.

References

Archer, D.: Orbital Forcing of Climate, available at: http://forecast.uchicago.edu/Projects/orbits.doc.html (last access: 24 September, 2013), 2013.

Belongie, S.: Rodrigues' Rotation Formula, in: MathWorld – a Wolfram Web Resource, created by: Weisstein, E. W., available at: http://mathworld.wolfram.com/RodriguesRotationFormula.html (last access: 12 September, 2013), 2013.

Berger, A.: Milankovitch theory and climate, Rev. Geophys., 26, 624–657, 1988.

Berger, A.: Comment on: "Insolation in terms of Earth's orbital parameters", by Rubincam, D. P., Theor. Appl. Climatol., 48, 195–202, 1994, Theor. Appl. Climatol., 53, 253–255, 1996.

Berger, A. and Loutre, M. F.:. Astronomical solutions for paleoclimate studies over the last 3 million years, Earth Planet. Sc. Lett., 111, 369–382, 1992.

Berger, A. and Loutre, M. F.: Precession, eccentricity, obliquity, insolation and paleoclimates, in: Long Term Climatic Variations, Data and Modelling, edited by: Duplessy, J. C. and Spyridakis, M. T., NATO ASI Series, 22, Springer, Berlin, Heidelberg, 107–151, 1994.

GMDD

6, 5947–5980, 2013

Berger, A., Loutre, M. F., and Tricot, C:. Insolation and Earth's orbital periods, J. Geophys. Res., 98, 10341–10362, 1993.
Berger, A., Loutre, M. F., and Gallee, H.: Sensitivity of the LLN climate model to the astronomical and CO_2 forcings over the last 200 kyr, Clim. Dynam., 14, 615–629, 1998.
Berger, A., Mélice, J. L., and Loutre, M. F.: On the origin of the 100-kyr cycles in the astronomical forcing, Paleoceanography, 20, PA4019, doi:10.1029/2005PA001173, 2005.
Berger, A., Loutre, M.-F., and Yin, Q.: Total irradiation during any time interval of the year using elliptic integrals, Quaternary Sci. Rev., 29, 1968–1982, 2010.
Berger, A. L.: Long-term variations of daily insolation and quaternary climatic changes, J. Atmos. Sci., 35, 2362–2367, 1978a.
Berger, A. L.: A Simple Algorithm to Compute Long Term Variations of Daily Insolation, Institut D'Astronomie et de Géophysique, Université Catholique de Louvain, Louvain-la Neuve, 18, 1978b.
Falkowski, P. G. and Godfrey, L. V.: Electrons, life and the evolution of Earth's oxygen cycle, Philos. T. Roy. Soc. B, 363, 2705–2716, 2008.
Falkowski, P. G. and Isozaki, Y.: Geology, the story of O_2, Science, 322, 540–542, 2008.
Falkowski, P. G., Katz, M. E., Milligan, A. J., Fennel, K., Cramer, B. S., Pierre Aubry, M., Berner, R. A., Novacek, M. J., and Zapol, W. M.: The rise of oxygen over the past 205 million years and the evolution of large placental mammals, Science, 309, 2202–2204, 2005.
Fröhlich, C.: Solar Constant: Construction of a Composite Total Solar Irradiance (TSI) Time Series from 1978 to present, Physikalisch-Meteorologisches Observatorium Davos, World Radiation Center, available at: http://www.pmodwrc.ch/pmod.php?topic=tsi/composite/SolarConstant (last access: 20 September 2013), 2013.
Hansen, J., Sato, M., and Ruedy, R.: Global Temperature Update Through 2012, NASA GISS, available at: http://www.nasa.gov/pdf/719139main_2012_GISTEMP_summary.pdf (last access: 20 November 2013), 2013.
Hays, J. D., Imbrie, J., and Shackleton, N. J.: Variations in the Earth's orbit: pacemaker of the Ice Ages, Science, 194, 1121–1132, doi:10.1126/science.194.4270.1121, 1976.
Huybers, P.: Early Pleistocene glacial cycles and the integrated summer insolation forcing, Science, 313, 508–511, 2006.
Imbrie, J., Boyle, E. A., Clemens, S. C., Duffy, A., Howard, W. R., Kukla, G., Kutzbach, J., Martinson, D. G., McIntyre, A., Mix, A. C., Molfino, B., Morley, J. J., Peterson, L. C., Pisias, N. G., Prell, W. L., Raymo, M. E., Shackleton, N. J., and Toggweiler, J. R.: On the structure and

GMDD
6, 5947–5980, 2013

origin of major glaciation cycles: 1. Linear responses to Milankovitch forcing, Paleoceanography, 7, 701–738, 1992.
Imbrie, J., Berger, A., Boyle, E. A., Clemens, S. C., Duffy, A., Howard, W. R., Kukla, G., Kutzbach, J., Martinson, D. G., Mcintyre, A., Mix, A. C., Molfino, B., Morley, J. J., Peterson, L. C., Pisias, N. G., Prell, W. L., Raymo, M. E., Shackleton, N. J., and Toggweiler, J. R.: On the structure and origin of major glaciation cycles 2. The 100,000-year cycle, Paleoceanography, 8, 699–735, 1993.
Joussaume, S. and Braconnot, P.: Sensitivity of paleoclimate simulation results to season definitions, J. Geophys. Res., 102, 1943–1956, doi:10.1029/96JD01989, 1997.
Jouzel, J., Masson-Delmotte, V., Cattani, O., et al.: EPICA Dome C Ice Core 800KYr Deuterium Data and Temperature Estimates, IGBP PAGES/World Data Center for Paleoclimatology Data Contribution Series, #2007-091, NOAA/NCDC Paleoclimatology Program, Boulder CO, USA, 2007a.
Jouzel, J., Masson-Delmotte, V., Cattani, O., Dreyfus, G., Falourd, S., Hoffmann, G., Minster, B., Nouet, J., Barnola, J. M., Chappellaz, J., Fischer, H., Gallet, J. C., Johnsen, S., Leuenberger, M., Loulergue, L., Luethi, D., Oerter, H., Parrenin, F., Raisbeck, G., Raynaud, D., Schilt, A., Schwander, J., Selmo, E., Souchez, R., Spahni, R., Stauffer, B., Steffensen, J. P., Stenni, B., Stocker, T. F., Tison, J. L., Werner, M., and Wolff, E. W.: Orbital and millennial Antarctic climate variability over the past 800,000 years, Science, 317, 793–797, 2007b.
Kasting, J.: How to Find a Habitable Planet, Princeton University Press, 2010.
Kasting, J. F., Whitmire, D. P., and Reynolds, R. T.: Habitable zones around main sequence stars, Icarus, 101, 108–128, 1993.
Kopp, G. and Lean, J. L.: A new, lower value of total solar irradiance: evidence and climate significance, Geophys. Res. Lett., 38, L01706, doi:10.1029/2010GL045777, 2011.
Kump, L. R., Kasting, J. F., and Crane, R. G.: The Earth System, Prentice Hall, San Francisco, 2010.
Laskar, J.: The limits of Earth orbital calculations for geological time-scale use, Philos. T. Roy. Soc. A, 357, 1735–1759, 1999.
Laskar, J., Robutel, P., Joutel, F., Gastineau, M., Correia, A. C. M., and Levrard, B.: A long-term numerical solution for the insolation quantities of the Earth, Astron. Astrophys., 428, 1, 261–685, doi:10.1051/0004-6361:20041335, 2004.
Laskar, J., Fienga, A., Gastineau, M., and Manche, H.: La2010: a new orbital solution for the long term motion of the Earth, arXiv, preprint arXiv:1103.1084, 2011.

GMDD
6, 5947–5980, 2013

Laskar, J.: Astronomical Solutions for Earth Paleoclimates, Institut de mecanique celeste et de calcul des ephemerides, available at: https://www.imcce.fr/Equipes/ASD/insola/earth/earth.html (last access: 25 April 2013), 2013.
Lisiecki, L. E. and Raymo, M. E.: A Pliocene–Pleistocene stack of 57 globally distributed benthic δ^{18}O records, Paleoceanography, 20, PA1003, doi:10.1029/2004PA001071, 2005.
Lisiecki, L. E., Raymo, M. E., and Curry, W. B.: Atlantic overturning responses to Late Pleistocene climate forcings, Nature, 456, 85–88, 2008.
Loutre, M. F., Paillard, D., Vimeux, F., and Cortijo, E.: Does mean annual insolation have the potential to change the climate?, Earth Planet. Sc. Lett., 221, 1–14, 2004.
Lüthi, D., Le Floch, M., Bereiter, B., et al.: EPICA Dome C Ice Core 800KYr Carbon Dioxide Data, IGBP PAGES/World Data Center for Paleoclimatology Data Contribution Series, #2008-055, NOAA/NCDC Paleoclimatology Program, Boulder CO, USA, 2008a.
Lüthi, D., Le Floch, M., Bereiter, B., Blunier, T., Barnola, J.-M., Siegenthaler, U., Raynaud, D., Jouzel, J., Fischer, H., Kawamura, K., and Stocker, T. F.: High-resolution carbon dioxide concentration record 650,000–800,000 years before present, Nature, 453, 379–382, doi:10.1038/nature06949, 2008b.
Meeus, J.: Astronomical Algorithms, Willmann-Bell, Richmond, VA, 1998.
Milankovitch, M.: Kanon der Erdbestrahlung und seine Anwendung auf das Eiszeitenproblem, 633 pp., Ed. Sp. Acad. Royale Serbe, Belgrade, (English translation Canon of Insolation and Ice Age Problem, Israel program for Scientific Translation; published for the US Department of Commerce and the National Science Foundation), 1941.
Muller, R. A. and MacDonald, G. J.: Glacial cycles and astronomical forcing, Science, 277, 215–218, 1997.
Rial, J. A.: Pacemaking the Ice Ages by frequency modulation of Earth's orbital eccentricity, Science, 285, 564–568, doi:10.1126/science.285.5427.564, 1999.
Rubincam, D. P.: Insolation in terms of Earth's orbital parameters, Theor. Appl. Climatol., 48, 195–202, 1994.
Sinnott, R. W.: Sky and Telescope, 70, p. 159, 1985.
Standish, E. M., Newhall, X. X., Williams, J. G., and Yeomans, D. K.: Orbital ephemerides of the Sun, Moon, and planets, in: The Astronomical Almanac, explanatory supplement, 279–323, 1992.

GMDD
6, 5947–5980, 2013

USNO: Selected Astronomical Constants, 2013, in: The Astronomical Almanac Online, US Naval Observatory, Washington, DC, available at: http://asa.usno.navy.mil/SecK/Constants.html (last access: 27 September 2013), 2013.

GMDD
6, 5947–5980, 2013

Table 1. Summary of constant and variable model input parameters.

Symbol	Constant/Variable	Value	Units	Reference	Notes
AU	Astronomical unit	149.597870700	10^6 km	USNO (2013)	–
a	Semi-major axis	149.59826114	10^6 km	Standish et al. (1992)	1.00000261 AU
T	Sidereal orbital period	365.256363	Days	Meeus (1998)	–
S_o	TSI at 1 AU	1366[a]	W m^{-2}	Fröhlich (2013)	Also see Kopp and Lean (2011)
e	Eccentricity	0.01670236[b]	–	La2004[c]	–
ε	Obliquity	23.4393[b]	degrees	La2004	–
$\tilde{\omega}$	Longitude of perihelion	102.9179[b]	degrees	La2004	–

[a] Users can change this default value.
[b] Default J2000 value. User can change these variables independently of each other or choose real astronomical solutions depending on the mode selected.
[c] La2004 refers to Laskar et al. (2004).

GMDD
6, 5947–5980, 2013

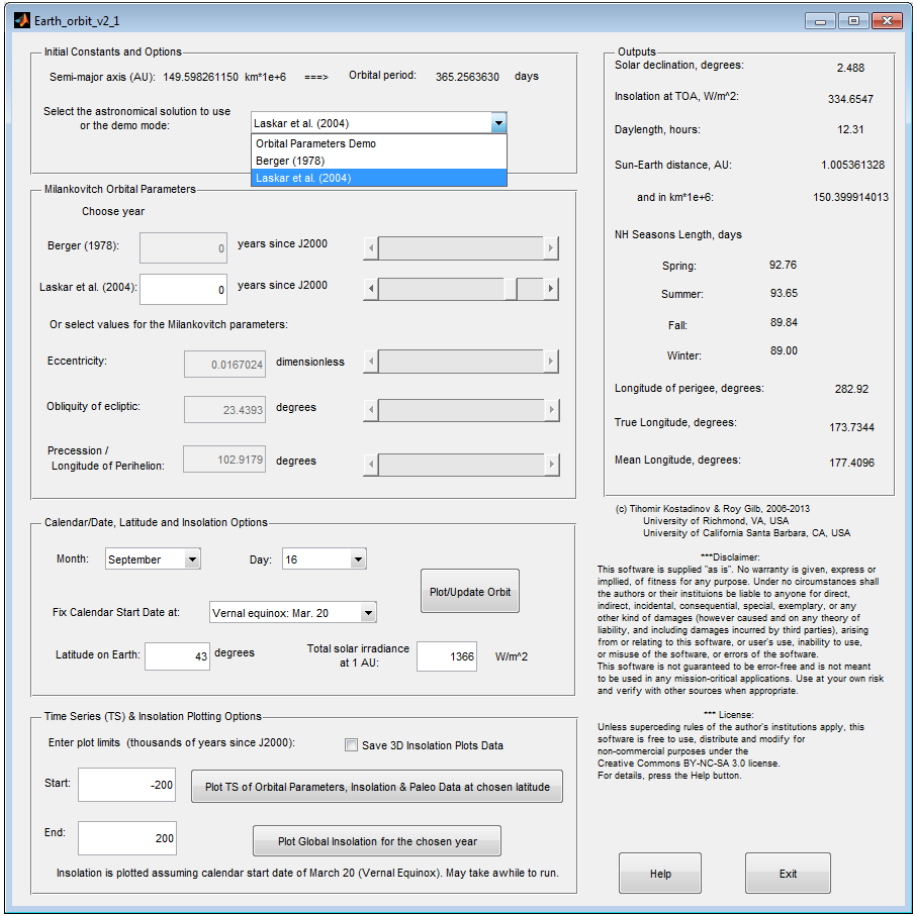

Fig. 1. Main MATLAB® GUI window of Earth Orbit v2.1. Input and output displayed is for 16 September, at 43° N latitude, at J2000, using the La2004 astronomical solutions.

GMDD
6, 5947–5980, 2013

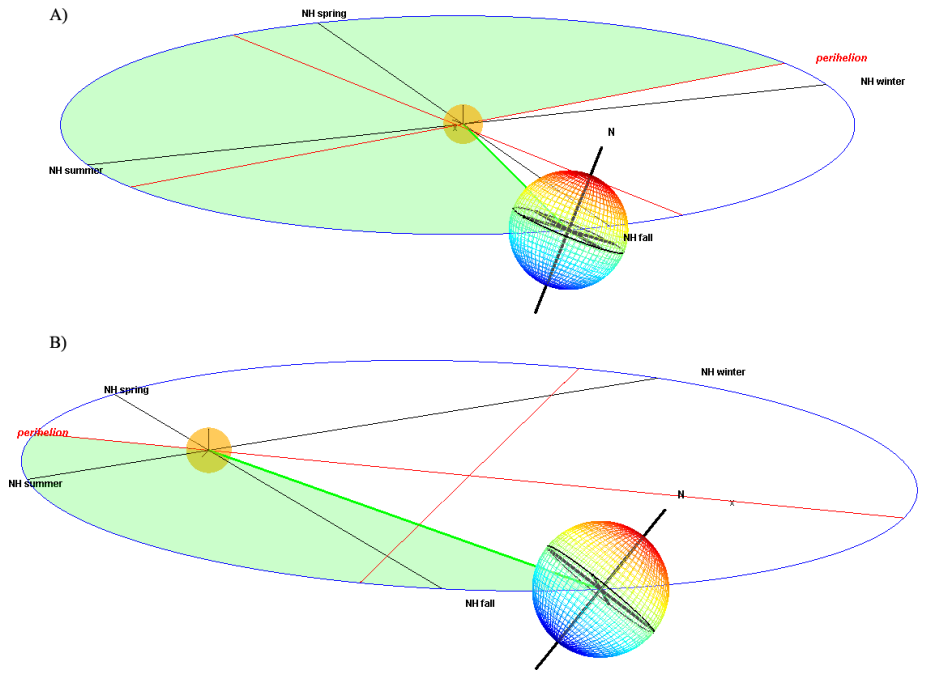

Fig. 2. (A) Present (J2000) orbital configuration for 16 September, and **(B)** demo orbital configuration for 1 July (Vernal equinox = 20 March), Eccentricity = 0.6, Obliquity = 45°, Longitude of perihelion = 225°. Note that the geometry is consistent with Berger et al. (2010), their Fig. 1, although it is being viewed from the direction of the fall equinox, as opposed to from the direction of spring equinox in their figure.

GMDD
6, 5947–5980, 2013

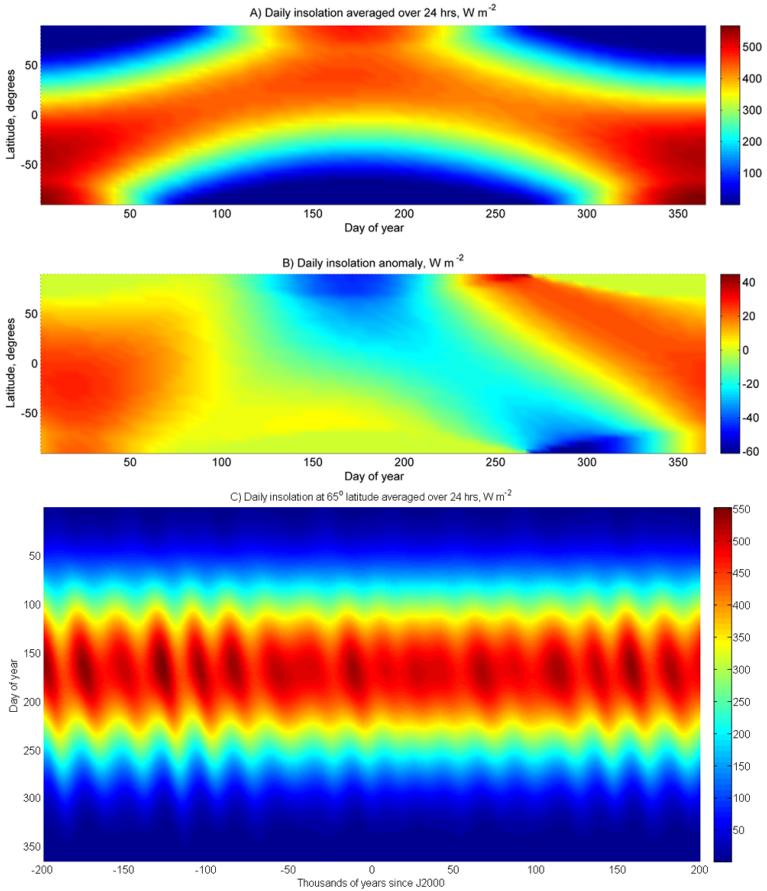

Fig. 3. (A) A day of year-latitude insolation plot for −115 Ky since J2000 and **(B)** the corresponding anomaly from J2000, using S_o = 1366 W m^{-2}. **(C)** Insolation time series at 65° N as a function of day of year, spanning ±200 kyr since J2000.

GMDD
6, 5947–5980, 2013

Earth Orbit v2.1

T. S. Kostadinov and R. Gilb

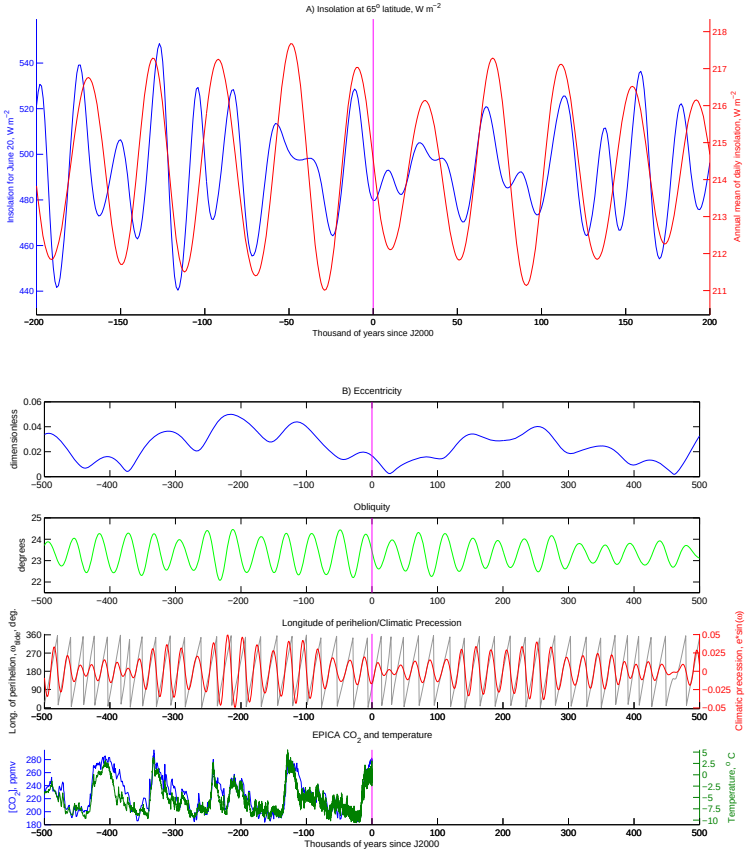

Fig. 4. (A) Insolation time series plot from −200 kyr to +200 kyr since J2000 at 65° N on 20 June (blue) and annual average (red). **(B)** Time series plots of Milankovitch orbital parameters and coincident paleoclimatic data from −500 kyr to +500 kyr since J2000. Panels from top to bottom display eccentricity, obliquity, longitude of perihelion and climatic precession, and EPICA ice core CO_2 and deuterium temperature.

GMDD
6, 5947–5980, 2013

T. S. Kostadinov and R. Gilb

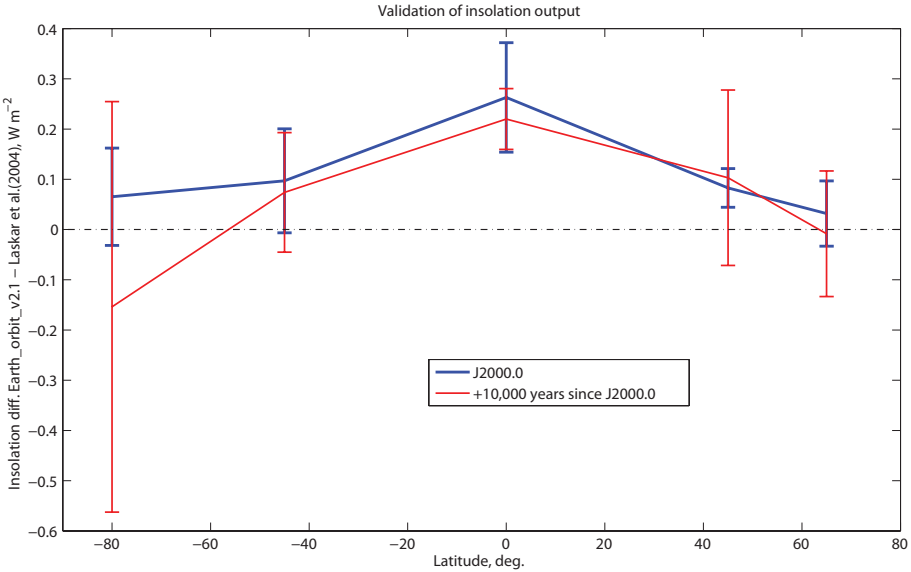

Fig. 5. Mean difference (W m^{-2}, error bars $\pm 1\sigma$, $N = 3$) between our insolation solution and the La2004 solution for several dates (22 March, 20 June, 22 December), as a function of latitude. Insolation computations use the model's own orbital geometry with no additional a priori input other than the Milankovitch parameter solutions of La2004. The La2004 solution was obtained from http://www.imcce.fr/Equipes/ASD/insola/earth/earth.html (Laskar, 2013).

GMDD
6, 5947–5980, 2013

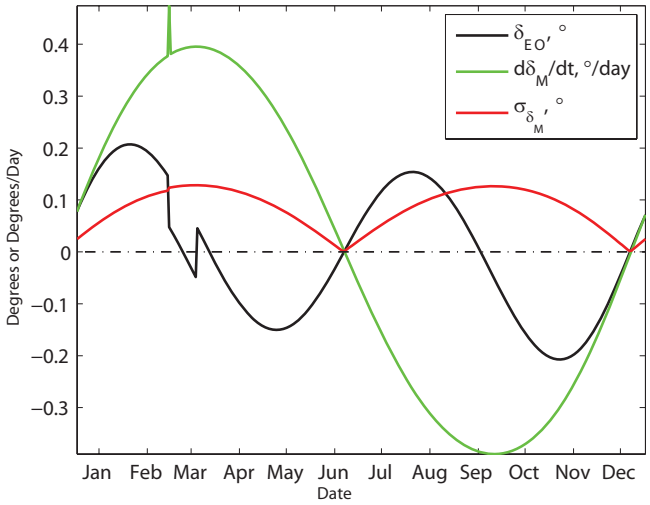

Fig. 6. Solar declination validation: difference between solar declination as computed by the internal geometry of the Earth orbit model and mean actual declination from the years 2009, 2010, 2011 and 2012 as computed for 12:00 UT for every day with the algorithms in Meeus (1998) (black solid line). The rate of change of declination (green solid line) and the standard deviation of declination for each date for the four years (red solid line, $N = 4$ for each data point) are also shown for reference. The model computations were performed with the calendar start date fixed at vernal equinox of 20 March. 29 February 2012 was removed from the analysis, so the abscissa corresponds to a given date, i.e. dates, not days of year were averaged for a given mean solar declination across the four years. Abscissa ticks represent the 15th of each month. If 00:00 UT is used for the Meeus computations instead, differences (black curve) have a different pattern and are larger, but never exceed $\sim 0.4^{\circ}$ (not shown).

GMDD
6, 5947–5980, 2013